*J. Fluid Mech.* (2002), *vol.* 451, *pp.* 421–443.  
DOI: 10.1017/S0022112001006681 Printed in the United Kingdom

# Force on a body in a continuously stratified fluid. Part 1. Circular cylinder

By EUGENY V. ERMANYUK
AND NIKOLAI V. GAVRILOV

Lavrentyev Institute of Hydrodynamics, 630090, Novosibirsk, Russia
e-mail: ermanyuk@hydro.nsc.ru

(Received 27 June 2000 and in revised form 25 July 2001)

This paper presents the force coefficients (added mass and damping) for a circular cylinder oscillating horizontally in a uniformly stratified fluid of limited depth and in a continuously stratified fluid with a smooth pycnocline. The frequency-dependent added mass and damping are evaluated from Fourier transforms of the experimental records of impulse response functions. The stratification is shown to have a strong effect on the fluid–body interaction. It is found that, when the characteristic vertical extent of stratification (depth of uniformly stratified fluid or pycnocline thickness) decreases, the power radiated with internal waves is reduced and the maximum of the frequency spectrum of wave power shifts toward lower frequency. The results of experiments are compared with available theoretical predictions.

## 1. Introduction

It is well known that rectilinear vibrations of a two-dimensional body at frequency $\omega$ in a stratified fluid with constant Brunt–Väisälä frequency $N$ produce internal waves within four beams (the so-called 'St.Andrew-cross-wave'), which are inclined at the angle $\varphi = \arcsin(\Omega)$ to the horizontal, where $\Omega = \omega/N$. The width of the beams is about the size of the oscillating body. In the three-dimensional case the internal waves radiated by a vibrating body are confined within a double cone. The phase pattern of internal waves, which was first identified in a pioneering study by Mowbray & Rarity (1967), can be explained from the viewpoint of 'ray' theory (see e.g. Turner 1973). However, the 'ray' theory fails to capture important physical values (such as the amplitude distribution across the internal wave beams, the decay of internal waves with distance, power radiated with waves, the force acting on a body oscillating in a stratified fluid), which are of vital practical interest in oceanography, atmospheric physics and marine engineering. A considerable scientific effort has been made during past three decades to gain more detailed knowledge of the internal wave field generated by different oscillatory disturbances. A detailed bibliography with critical assessment of existing wave theories and solutions to a variety of three-dimensional problems can be found in Voisin (1991). Particular mention should be made of the solutions for the flat plate (Hurley 1969), the spheroid (Lai & Lee 1981), the sphere (Appleby & Crighton 1987), and circular (Appleby & Crighton 1986; Makarov, Neklyudov & Chashechkin 1990) and elliptic cylinders (Hurley 1997; Hurley & Keady 1997). Note that the measurements and observations of the internal wave patterns generated by oscillating bodies do not seem to provide a decisive verification of existing wave theories (see e.g. discussions in Ivanov 1989 and Makarov

*et al.* 1990). Recent advancement in detailed quantitative measurement of parameters of internal wave motion has been attained with the help of the 'synthetic schlieren' technique described in Sutherland *et al.* (1999) and Dalziel, Hughes & Sutherland (2000).

An alternative approach is to compare the measurements of the force acting on a body oscillating in a stratified fluid to the predictions of a particular internal wave theory. Apart from the purposes of verification, this problem has an engineering counterpart in the prediction of the low-frequency motion of marine structures and deep submersibles in real stratified sea. However, few authors have paid attention to this problem. Within the framework of the Boussinesq approximation, Lai & Lee (1981) have obtained a solution for a spheroid oscillating in the vertical direction in inviscid infinitely deep stratified fluid with $N = \text{const}$. Under the same assumptions, Hurley (1997) has derived the formula for the hydrodynamic force acting on an elliptic cylinder undergoing rectilinear vibrations at an arbitrary angle to the horizontal. Lai & Lee (1981) formulate their results by introducing the notion of the complex added mass and consider its amplitude and phase versus the oscillation frequency. A similar concept is used by Hurley (1997). These results can be easily reformulated in terms of the standard added mass and damping coefficient, i.e. the total hydrodynamic force can be decomposed into the components acting in phase with acceleration and velocity of the body motion as is customary in ship hydrodynamics (see e.g. Newman 1977, 1978). The added mass characterizes the variation of inertial properties of the fluid–body system while the damping coefficient is proportional to the mean dissipated power. In ideal linearly stratified fluid, the radiation of energy with waves is the sole mechanism of energy dissipation. Accordingly, the damping coefficient is non-zero only when $\Omega < 1$ both in two-dimensional and three-dimensional problems since the radiation of internal waves in such a system at $\Omega > 1$ is physically impossible. When $\Omega > 1$, the added mass asymptotically approaches the value in homogeneous fluid. The behaviour of the added mass at $\Omega < 1$ in two-dimensional and three-dimensional cases is quite different. Lai & Lee (1981) show that the added mass of a vertically oscillating spheroid is logarithmically infinite when $\Omega \to 0$ and drops to zero at $\Omega = 1$, while, according to Hurley's (1997) solution, the added mass of a circular cylinder is identically zero for $\Omega \leqslant 1$. Hurley & Keady (1997) have generalized Hurley's (1997) solution to take viscous effects into account. It follows from their theory that Hurley's (1997) solution is expected to hold approximately for the viscous case at sufficiently large Reynolds numbers, which are normally encountered in experiment. At the same time, for obvious physical reasons, the effects due to viscosity are expected to cause non-zero damping at $\Omega > 1$. Ermanyuk (2000) has evaluated experimentally the added mass and damping of an oscillating circular cylinder in a deep linearly stratified fluid. The measured values are found to be in a good agreement with Hurley's (1997) solution.

Mention should be made of the work done by Gorodtsov & Teodorovich (1986). They have evaluated the mean power radiated by an oscillating body in a stratified fluid. However, their results are found to be in disagreement with the results obtained in Hurley (1997) and Lai & Lee (1986). The disagreement is due to the assumption that a body in a continuously stratified fluid can be modelled by the distribution of singularities obtained from the solution of the same problem in ideal homogeneous fluid. At the same time, the results presented in Gorodtsov & Teodorovich (1986) can be easily corrected once a correct distribution of singularities is known. In the present paper we make use of their approach in combination with the recent results obtained in Voisin (2001*b*).

It should be noted that, for the sake of simplicity, in the major part of the above-mentioned theoretical studies the fluid is assumed to be infinitely deep, inviscid and having constant Brunt–Väisälä frequency. Therefore, an investigation of more realistic and general types of stratification is of considerable interest. Notable progress in this direction has been attained in the experimental research on the drag on a body moving horizontally at constant velocity in a stratified fluid (the so-called 'dead water' phenomena). The drag on a sphere has been measured in a two-fluid system with interface (Nikitina 1959), linearly stratified fluid (Lofquist & Purtell 1984), and a thermocline (Shishkina 1996). Shishkina (1996) also presents a comparative analysis of the drag coefficients for a sphere for different profiles of stratification. The measurements of the drag on a two-dimensional body include the case of mountain-shaped profiles in linearly stratified fluid (Castro, Snyder & Baines 1990) and a circular cylinder in thermocline (Arntsen 1996).

In the present investigation we consider the force acting on two- and three-dimensional bodies oscillating horizontally in a continuously stratified fluid. The cases of a circular cylinder and a sphere provide clues to the understanding of the main effects in two-dimensional and three-dimensional problems, respectively. We focus our attention on two typical cases of stratification: (*a*) linearly stratified fluid of limited depth, (*b*) a smooth density profile with homogeneous upper and lower layers and a layer of high density gradient (pycnocline) in between. Thus, we can compare the dynamical properties of these two types of wave guides. The qualitative difference between the phase patterns of internal waves propagating within these two types of wave guides can be predicted by 'ray' theory. In particular, the literature on the reflection of internal waves at rigid boundaries in linearly stratified fluid is reviewed in Turner (1973). A detailed recent study of this problem can be found in Kistovich & Chashechkin (1995). The evolution of internal waves produced by a vibrating cylinder in the case of thermocline stratification is described in Nicolaou, Liu & Stevenson (1993).

The experimental technique used in the present investigation is analogous to the one described in Ermanyuk (2000). The theoretical background is based on the important paper by Cummins (1962) (see also Wehausen 1971 for an overview and Kerwin & Narita 1965 for a pioneering experimental study). Following this approach, we make use of experimental records of damped oscillations of a body (impulse response functions) in a stratified fluid and Fourier-transform the problem from the time- to the frequency-domain in order to evaluate the frequency-dependent dynamic coefficients, namely added mass and damping. The first detailed analysis of the dynamic effects due to stratification on the dynamics of oscillatory motion of a submerged body was executed in the time-domain (Larsen 1969). Larsen (1969) gives the solution to the problem of the damped oscillations of a sphere and circular cylinder (in the latter case, the final result without detailed proof) initially displaced from the equilibrium position in a linearly stratified fluid. In the present investigation, we apply Fourier transforming from the time- to the frequency-domain not only to the experimental data but also to Larsen's (1969) results and show that they exactly coincide with those obtained by Hurley (1997) and by Lai & Lee (1981) for the cases of vertical oscillations of a circular cylinder and a sphere, respectively. We also present some notes on the application of the Kramers–Kronig relations (see Kotik & Mangulis 1962; Wehausen 1971) which are used effectively in many problems of body oscillations in surface waves (see e.g. McIver & Linton 1991). In particular, when applied to Hurley's (1997) solution, these relations require a modification as compared to their popular form (Wehausen 1971) in strict accordance with Landau & Lifshitz (1980).

The present investigation consists of two parts. In Part 1, the present paper, we consider the oscillations of a circular cylinder in a continuously stratified fluid. The theoretical background of the experimental method is described in § 2. In § 2 we also define the non-dimensional force coefficients and discuss the application of the Kramers–Kronig relations to the frequency-dependent added mass and damping. The description of the experimental installation is given in § 3. In § 4 we present the results of experiments and their discussion.

Part 2, a subsequent paper, is dedicated to the case of a sphere. There we discuss the particularities of the three-dimensional problem for the same types of stratification as in Part 1 and, in particular, present an experimental verification of the solution for the force acting on a horizontally oscillating sphere in infinitely deep stratified fluid with $N = \text{const}$ recently obtained by Voisin (2001*a*).

## 2. Theoretical background

Let us assume that a body performing small oscillations in a continuously stratified fluid can be idealized as a linear system. It is well known that, once the response of any stable linear system to a unit impulse $r(t)$ is known, the response of the system to an arbitrary force $f(t)$ may be written as the convolution integral

$$x(t) = \int_0^\infty r(\tau) f(t-\tau)\,\mathrm{d}\tau. \tag{2.1}$$

In the case of harmonic forcing with frequency $\omega$

$$f(t) = f_0 \exp(\mathrm{i}\omega t), \tag{2.2}$$

and substituting (2.2) in (2.1) one obtains

$$x(t) = f_0 \exp(\mathrm{i}\omega t) R(\omega), \tag{2.3}$$

where the complex frequency response function $R(\omega)$ is defined as Fourier transform of the impulse response function

$$R(\omega) = \int_0^\infty r(\tau) \exp(-\mathrm{i}\omega\tau)\,\mathrm{d}\tau.$$

Let us separate the complex frequency response function into real and imaginary parts as $R(\omega) = R_c(\omega) - \mathrm{i}R_s(\omega)$, where

$$R_c = \int_0^\infty r(\tau)\cos(\omega\tau)\,\mathrm{d}\tau, \quad R_s = \int_0^\infty r(\tau)\sin(\omega\tau)\,\mathrm{d}\tau.$$

Furthermore, for the sake of clear physical representation, we introduce the amplitude $|R| = ([R_c]^2 + [R_s]^2)^{1/2}$ and the phase $\theta = \arctan(R_s/R_c)$ of the frequency response function. In the general case of an arbitrary exciting force the motion of a body emitting waves can be mathematically described by an integro-differential equation containing a convolution integral, which takes into account the 'memory' effects. However, for the particular case of harmonic excitation, the equation of body motion in one degree of freedom reduces to the second-order linear differential equation with frequency-dependent coefficients (see Cummins 1962; Wehausen 1971), which can be written as follows:

$$(M + \mu(\omega))\frac{\mathrm{d}^2x}{\mathrm{d}t^2} + \lambda(\omega)\frac{\mathrm{d}x}{\mathrm{d}t} + cx = f_0 \exp(\mathrm{i}\omega t). \tag{2.4}$$

Here, $M$ is the inertia of a body, $\mu(\omega)$ is the added mass, $\lambda(\omega)$ is the damping coefficient, and $c$ is the restoring force coefficient. In what follows, we restrict our consideration to the case of stable systems, i.e. we assume $c > 0$. Combining (2.3) and (2.4) and using linearity of the system one can write the formulas for frequency-dependent coefficients

$$\mu(\omega) = \frac{c}{\omega^2}\left(1 - \frac{|R(0)|}{|R(\omega)|}\cos(\theta(\omega))\right) - M, \tag{2.5}$$

$$\lambda(\omega) = \frac{c}{\omega}\frac{|R(0)|}{|R(\omega)|}\sin(\theta(\omega)). \tag{2.6}$$

Here $|R(0)|$ denotes the amplitude of the frequency response function at zero frequency. Note that for a unit impulse $cR(0) = 1$, which follows from substituting (2.3) in (2.4) and setting $\omega = 0$. The use of experimental records obtained for an arbitrary value of the impulse necessitates the normalization of $|R(\omega)|$ by $|R(0)|$. This technique is applicable to any linear system regardless of its physical nature provided the condition of causality is satisfied. In particular, this approach can be applied to prove the identity of time-domain (Larsen 1969) and frequency-domain (Hurley 1997; Lai & Lee 1981) solutions to the problem of the vertical oscillations of a circular cylinder and a sphere in unbounded stratified fluid with constant Brunt–Väisälä frequency $N$. The Brunt–Väisälä frequency is defined as $N(y) = (-g\,\mathrm{d}\rho/\rho\,\mathrm{d}y)^{1/2}$, where $\rho(y)$ is the fluid density, the $y$-axis is directed vertically upwards, and $g$ is the gravity acceleration. An interested reader can find details concerning the relation between the time- and frequency-domain solutions in Appendix A.

It is important to note that the added mass $\mu(\omega)$ and damping coefficient $\lambda(\omega)$ are related to each other by the Kramers–Kronig relations. The derivation of these relations is presented in detail in Landau & Lifshitz (1980). The Kramers–Kronig relations relate the real and imaginary parts of any complex function of the frequency $\omega$, which is analytic in one half of the complex $\omega$-plane. In the theory of ship motions, the relevance of the Kramers–Kronig relations to the function $\mu(\omega) - \mathrm{i}\lambda(\omega)/\omega$ was first recognized by Kotik & Mangulis (1962). As emphasized in Landau & Lifshitz (1980) and Kotik & Mangulis (1962), relations of Kramers–Kronig type are to be expected whenever there is linearity and causality. In the present study the causal function is the impulse response $r(t)$ and the frequency responce $R(\omega)$ plays the role of the so-called susceptibility (see Landau & Lifshitz 1980), which represents the ratio of harmonic response to harmonic forcing. As is evident from (2.5) and (2.6), the added mass and damping are simply related to the Fourier-image of the causal function of time. Correspondingly, the function $\mu(\omega) - \mathrm{i}\lambda(\omega)/\omega$ is analytic in the lower part of the complex $\omega$-plane. The singularities of this function are the zeros of $R(\omega)$, which are all in the upper part of the $\omega$-plane, and, in some cases, the origin $\omega = 0$. In particular, the singularity at $\omega = 0$ is present in Hurley's (1997) solution. Following Landau & Lifshitz (1980) we can write, in our notation,

$$\mu(\omega) - \mu(\infty) = \frac{2}{\pi}\int_0^\infty \lambda(\alpha)\frac{\mathrm{d}\alpha}{\alpha^2 - \omega^2}, \tag{2.7}$$

$$\lambda(\omega) = -\frac{2}{\pi}\omega^2\int_0^\infty [\mu(\alpha) - \mu(\infty)]\frac{\mathrm{d}\alpha}{\alpha^2 - \omega^2} + \lambda(0). \tag{2.8}$$

Here $\mu(\infty)$ is the limit of added mass at $\omega \to \infty$ and the integrals are Cauchy principal-value integrals. The above expressions are different from those given in Wehausen

(1971) in the presence of the last term in (2.8), which takes into account the simple pole of $\mu(\omega) - \mathrm{i}\lambda(\omega)/\omega$ at $\omega = 0$. There are reasons to believe that the singularity at $\omega = 0$ appears not only in Hurley (1997) but also in other two-dimensional problems of body oscillations in continuously stratified fluid. The proof of the Kramers–Kronig relations for the solution given in Hurley (1997) is presented in Appendix B. Let us also note that with the experimental technique used in the present paper the Kramers–Kronig relations are fulfilled automatically (to within the accuracy of the experiments).

It should be also noted that the presence of the singularity at zero frequency in the function $\mu(\omega) - \mathrm{i}\lambda(\omega)/\omega$ makes it necessary to introduce a correction of another popular formula for the added mass coefficient (see Wehausen 1971), which requires zero value of the integral

$$\int_0^\infty [\mu(\omega) - \mu(\infty)]\,\mathrm{d}\omega. \tag{2.9}$$

However, the value of the integral (2.9) is non-zero for the solution presented in Hurley (1997) (for details see Appendix B). A similar result is expected for other two-dimensional problems in continuously stratified fluid. Note, however, that in three-dimensional problems the formulas (2.7), (2.8) can be used in their standard form (Wehausen 1971) since the singularity at $\omega = 0$ does not occur. Accordingly, the integral (2.9) takes a zero value.

The Kramers–Kronig relations and their consequences give an efficient test for the validity of numerical and experimental results. They can also be effectively used in the methods aimed at the evaluation of the mean power radiated with waves (see e.g. Hurley 1969; Gorodtsov & Teodorovich 1986). Multiplying (2.4) by $\mathrm{d}x/\mathrm{d}t$ then integrating and taking an average over a period of oscillations, one can immediately obtain that the mean dissipated power is $P(\omega) = a^2\omega^2\lambda(\omega)/2$, where $a$ is the amplitude of harmonic oscillations. Thus, once the power $P(\omega)$ is known, it is easy to reconstruct the damping coefficient $\lambda(\omega)$ and the added mass $\mu(\omega)$.

In the above considerations we have discussed the general properties of the added mass and damping coefficients in the context of the 'inviscid linear scenario' when the hydrodynamic loading is governed by wave effects. In this case, there is only one dynamically important dimensionless parameter $\Omega = \omega/N$, which plays the role of a Froude number. For a cylinder of diameter $D$ oscillating in a continuously stratified fluid, it is convenient to introduce the non-dimensional added mass and damping coefficients as follows:

$$C_\mu = \mu/\rho_c S, \tag{2.10}$$

$$C_\lambda = \lambda/\rho_c S N, \tag{2.11}$$

where $\rho_c$ is the fluid density at the depth corresponding to the cylinder centre, and $S = \pi D^2/4$ is the cross-sectional area. The choice of the background scaling frequency $N$ for parameter $\Omega$ and damping coefficient $C_\lambda$ defined by (2.11) is obvious for a uniformly stratified fluid with $N = \mathrm{const}$. For an arbitrary distribution of the buoyancy frequency over depth, it is natural to choose either the global cut-off frequency for wave effects $N = N_m = \max[N(y)]$ or the local cut-off frequency at the vertical coordinate $y_c$ of the cylinder centre so that $N = N_c = N(y_c)$. In the present study the geometric set-up for experiments in the pycnocline is chosen so that $N = N_m = N_c$. Correspondingly, $\Omega = \omega/N_m$ and $C_\lambda = \lambda/\rho_c S N_m$. The definition of the added mass coefficient (2.10) is appropriate for any type of stratification.

With the added mass and damping coefficients defined as in (2.10) and (2.11),

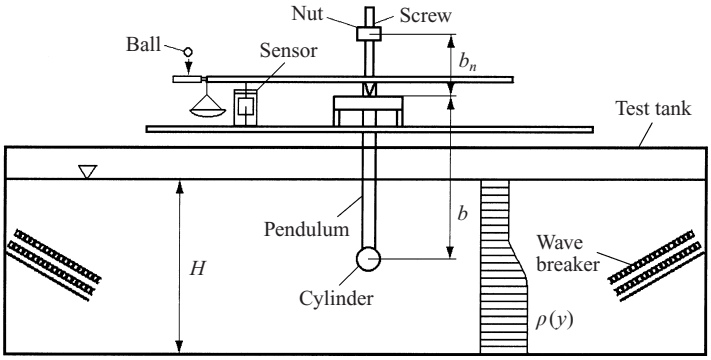


FIGURE 1. Experimental setup.

Hurley's (1997) solution for the force acting on a circular cylinder oscillating in an unbounded uniformly stratified fluid is $C_\mu \equiv 0$, $C_\lambda = (1-\Omega^2)^{1/2}$ for $\Omega < 1$, and $C_\mu = (1-\Omega^{-2})^{1/2}$, $C_\lambda \equiv 0$ for $\Omega > 1$. It should be noted that these expressions are independent of the direction of oscillations. In what follows, Hurley's (1997) solution serves as the infinite-depth limit for the analysis of the effects caused by the limited vertical extent of stratification.

The non-dimensional oscillation amplitude $a/D$ characterizes the nonlinearity of the problem both for wave and viscous effects. In the present experiments this parameter was sufficiently small ($a/D < 0.1$) that there were no detectable nonlinear effects to within the accuracy of the experiments.

To complete the parametrization of the problem, we need to take into account the effects due to viscosity. The in-line force coefficients for a circular cylinder oscillating in a homogeneous fluid are known to be the functions of the Keulegan–Carpenter and Stokes numbers (see Sarpkaya 1986). In the case of harmonic oscillations, the Keulegan–Carpenter number is equivalent to $a/D$. The Stokes number is usually introduced as $\beta = D^2\omega/\nu$, where $\nu$ is kinematic viscosity. The role of this parameter will be discussed in §4.1 dedicated to experiments in homogeneous fluid. For a stratified fluid, it is convenient to introduce the 'internal' Stokes number $\beta_N = \beta/\Omega = D^2N/\nu$. Finally, the functions sought in the present experimental study can be formulated as $C_\mu = C_\mu(\Omega)$, $C_\lambda = C_\lambda(\Omega)$ measured at certain values of $\beta_N$ for a given geometric set-up of the experiments. The set of non-dimensional geometric parameters reduces to $H/D$ for linearly stratified fluid, where $H$ is the fluid depth, and $\delta/D$ for the pycnocline, where $\delta$ is the characteristic pycnocline thickness. The centre of the cylinder in all experimental runs was submerged to the depth $H/2$. In experiments with the pycnocline the total depth of fluid $H$ was sufficiently large to be considered infinite.

## 3. Experimental arrangement

The experimental technique used in the present study is similar to Ermanyuk (2000), where one can find detailed descriptions. In what follows, we restrict our description to the most essential points. The experiments were carried out in a test tank (0.15 m wide, 0.38 m deep and 2.3 m long). The schematic of the experimental installation is shown in figure 1. The damped oscillation tests were performed with the help of a cross-shaped pendulum. A circular cylinder of diameter $D = 3.7$ cm was attached to the lower end of the pendulum. The gaps between the ends of the cylinder

and the sidewalls of the tank were equal to 0.5 mm. The volume of the immersed streamlined part of the pendulum was less than 1% of the cylinder volume. The upper part of the pendulum had a micrometric screw with a nut of mass $m_n = 188$ g. The variation of the vertical coordinate of the nut $b_n$ allowed the restoring moment of the pendulum to be changed. The distance between the point of rotation of the pendulum and the centre of the cylinder was $b = 60$ cm. The maximum magnitude of the horizontal displacement of the cylinder in experimental runs did not exceed $0.1D$. The moment of inertia of the pendulum $I_0$ (without nut) was measured with an accuracy of 0.5%, the measured value being $I_0 = 1.12 \times 10^6$ g cm$^2$. The total moment of inertia is $I = I_0 + m_n b_n^2$. Correspondingly, the value of the inertial term in the equation of the rectilinear motion (2.4) and formulas (2.5), (2.6) is $M = I/b^2$. The oscillations of the pendulum were induced by dropping a steel ball on a pre-tensioned rubber membrane attached to the end of the horizontal bar of the pendulum. The history of damped oscillations was measured by an electrolitic sensor whose output was sampled at 20 Hz with a 12-bit analog-to-digital convertor. The restoring force coefficient $c$ was evaluated from static calibration *in situ* by loading a light bowl at the end of the horizontal bar of the pendulum with standard calibrated weights. The accuracy of static calibration was about 0.5%. Because of the high sensitivity of the experimental system, special care was taken to protect it from mechanical vibrations and air currents. To prevent the reflection of waves at the ends of the test tank, we used two types of wave-absorbing devices. In the case of linear stratification the wave energy of incident internal waves was effectively dissipated by perforated flat plates installed parallel to the end of the test tank. In experiments with a pycnocline the wave-energy absorber represented a 'sandwich' of two perforated flat plates and an opaque plate, inclined at a small angle to horizontal. The performance of the wave absorbers proved to be sufficiently effective.

A weak solution of glycerine (linear stratification) or sugar (pycnocline) in water was used to produce a prescribed density distribution. Linear stratification was created by slowly filling the test tank with several layers of fluid having a prescribed density difference between the layers. The thickness of one layer was about 1.5–2 cm. Within two days, the layered structure eventually disappeared due to diffusion. The linearity of the resulting density distribution was checked by a conductivity probe calibrated over samples of known density. These data were used to evaluate the Brunt–Väisälä frequency.

A smooth density profile with a pycnocline was created by filling the test tank with two layers of miscible fluids. Owing to diffusion, the initial sharp interface between the layers evolved into a smooth density profile. In the coordinate system with the origin taken at the free surface and the $y$-axis directed vertically upwards the measured density distribution over depth fitted the following approximation:

$$\rho(y) = \rho_0 \left[1 - \frac{\epsilon}{2} \tanh\left(\frac{2(y+h)}{\delta}\right)\right], \quad \rho_0 = \frac{\rho_1 + \rho_2}{2}, \quad \epsilon = \frac{\rho_2 - \rho_1}{\rho_1},$$

where $h$ is the depth of the upper layer (in experiments $h = H/2$), $\delta$ is the characteristic thickness of the pycnocline, and $\rho_1$ and $\rho_2$ are the fluid densities in the upper and lower layers, respectively. According to the theoretical solution for the problem of diffusion of a weak admixture (see, for example, Landau & Lifshitz 1987) the density profile is described by an error function. However, in the Taylor series for an error function and for a hyperbolic tangent the first two terms coincide while the third terms differ by only 25%. As result, both functions provide good approximations

to the experimental data. However, from a practical point of view, the use of a simple analytical function, such as a hyperbolic tangent, is more convenient. In accordance with theoretical predictions the characteristic thickness of the pycnocline increases with time as $\delta \sim t^{1/2}$. Owing to the low diffusion rate of sugar in water, the characteristic time scale of this growth is measured by days. There was no detectable increase of $\delta$ within the few hours needed to perform a series of experiments. To study a sufficiently broad range of non-dimensional frequencies $\Omega$ for different values of $\delta/D$ as well as the effects due to variation of $\beta_N$, the experiments were performed for several values of $\epsilon$ ($\epsilon = 0.003; 0.006; 0.009$).

Because of instrument noise, reliable experimental estimates of the frequency-dependent coefficients may be obtained in a certain frequency range in the vicinity of the frequency $\omega_*$ corresponding to the resonant peak of $|R(\omega)|$. To study the whole frequency range of interest, it is necessary to perform a series of experiments for a set of $\omega_*$ and match the results on a common plot so that the data obtained at different $\omega_*$ overlap. The variation of $\omega_*$ can be easily attained by variation of the restoring force coefficient $c$. For each set of experimental conditions we recorded about a dozen impulse response functions at different $c$.

## 4. Experimental results

### 4.1. *Homogeneous water*

The experiments in homogeneous water were performed to obtain background information on the behaviour of added mass and damping for a circular cylinder oscillating in a viscous fluid of limited depth. There exists an extensive literature on the force coefficients for a circular cylinder submerged in oscillatory flow of viscous fluid. The ongoing research activity in this field is motivated by the important practical problem of dynamical interaction between marine structures and the ocean environment. As a result, most reported experiments have been performed under conditions corresponding to relatively high values of the Keulegan–Carpenter and Stokes numbers. A particular case of low Keulegan–Carpenter numbers is considered in Sarpkaya (1986). However, the range of non-dimensional parameters, which is of interest in the present study, and, in particular, the effect of limited depth $H$, has not yet been studied. In addition, the present experiments in homogeneous water were motivated by the necessity to cut out unwanted free-surface effects. In a sufficiently long test tank, the natural period of free oscillations of water (period of seiches) can be close to the frequency of the pendulum oscillations $\omega_*$. As this takes place, the energy of the pendulum oscillations is gradually transferred into the energy of seiche waves (at the time scale of several periods $2\pi/\omega_*$) and vice versa. For the pendulum motion, one observes a typical pattern of beating. In this case, the processing of an experimental record according to (2.5), (2.6) shows discontinuities for the curves $\mu(\omega)$ and $\lambda(\omega)$, which are localized in a narrow frequency band in the vicinity of the frequency of seiche motion. To filter out this effect, for each value of water depth $H$ the length of the fluid volume in the test tank was limited by insertion of endwalls so that the seiche frequency was twice the highest frequency studied in experiments. Under this condition, there was no detectable interference with the free-surface effects. The free surface could be considered as a rigid lid.

Experiments in homogeneous water can be interpreted within the framework of the classic Stokes asymptotic theory of oscillatory motion in homogeneous viscous fluid under assumptions $a/D \ll 1$ and $\beta \gg 1$ (see Stokes 1851; Wang 1968; Landau

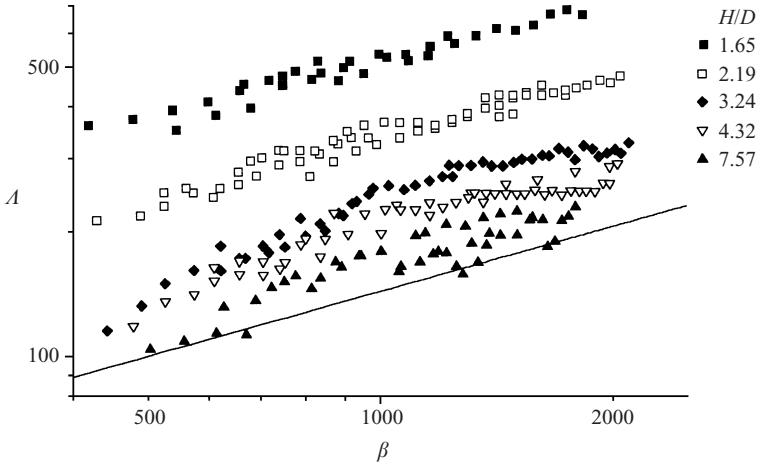


FIGURE 2. Non-dimensional damping $\Lambda$ vs. Stokes number $\beta$ for homogeneous fluid of limited depth. Solid line: formula (4.1).

& Lifshitz 1987). For a cylinder oscillating in unbounded viscous fluid this theory predicts the following values of the added mass and damping coefficients per unit length:

$$\mu = \rho S, \quad \lambda = \pi\sqrt{2}\eta\beta^{1/2}, \tag{4.1}$$

where $\eta = \rho\nu$ is the dynamic viscosity of the fluid.

The present experiments were conducted for a set of non-dimensional water depths $H/D = 7.57, 4.32, 3.24, 2.19, 1.65$. It is found that the added mass coefficient of the cylinder depends only on the depth of fluid. The mean measured values are $C_\mu = 1.05$, 1.12, 1.24, 1.54, 2.25, respectively. The scatter of the experimental points about the mean values of $C_\mu$ does not exceed $\pm 4\%$. It is interesting to compare the measured values with the results of numerical calculations of $C_\mu$ based on the model of ideal homogeneous fluid of limited depth (the free surface is idealized as a rigid lid). For the experimental values of $H/D$, calculations performed with the help of a computer code developed by Professor I. V. Sturova yield the following values: $C_\mu^{ideal} = 1.03$, 1.09, 1.17, 1.41, 1.87. The difference between $C_\mu$ and $C_\mu^{ideal}$ systematically increases for lower values of $H/D$.

The values of the damping coefficient $\Lambda = \lambda/\eta$ versus $\beta$ for different $H/D$ are plotted in figure 2 on a logarithmic scale. It is easy to see that for all values of the fluid depth $H/D$ the law $\Lambda \sim \beta^{1/2}$ is well satisfied. The effect of fluid depth on $\Lambda$ is pronounced when $H/D < 3.24$ although it is detectable at higher $H/D$. It should be noted that for large $H/D$, for example, at $H/D = 7.57$ when the effect of limited depth is supposed to be negligible, the damping coefficient $\Lambda$ is somewhat greater than predicted by (4.1). The disagreement is believed to be caused by the relatively low value of $\beta$ in experiments and by the effect of the flow in the gaps between the ends of the cylinder and the walls of the tank.

For the purpose of explicit quantitative comparison, the results of experiments in homogeneous water are also presented in terms of $C_\lambda(\Omega)$ together with the experimental data obtained in linearly stratified fluid. In this case the normalization of $\lambda$ measured in homogeneous water by the wave damping scale $\rho_c SN$ has a purely formal sense.

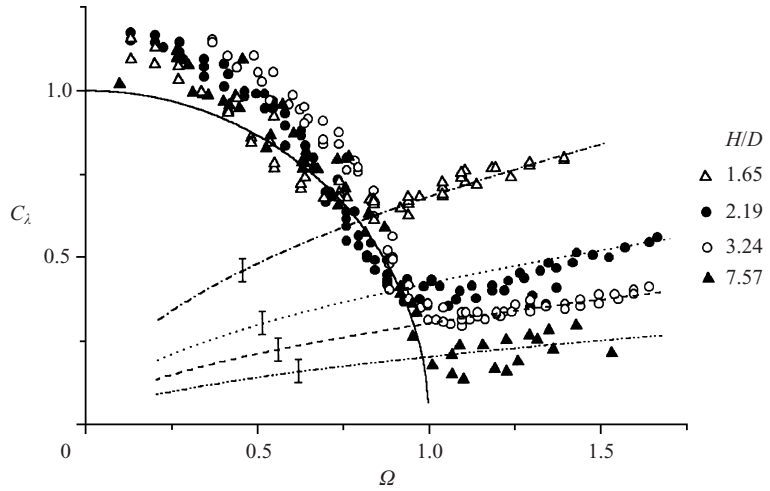


FIGURE 3. Damping coefficient $C_\lambda$ *vs.* frequency $\Omega$ in linearly stratified fluid: solid line, theory for $H/D = \infty$ (Hurley 1997). Other lines show experimental data obtained in homogeneous fluid for $H/D = 1.65$ (–·–), 2.19 (···), 3.24 (– – –), 7.57 (–··–). Vertical bars denote the scatter of experimental data. Experimental data for $H/D = 7.57$ shown in figures 3, 4 and 5 are taken from Ermanyuk (2000).

### 4.2. *Linear stratification*

The effect of limited depth for linearly stratified fluid was studied at $H/D = 1.65$, 2.19, 3.24. The values of the Brunt–Väisälä frequency were $N = 0.9$, 0.85, 0.9 rad s$^{-1}$, respectively. The difference between the actual values of $N$ at different $H/D$ is sufficiently small to be safely neglected. For better insight in the large-depth limit, we also use the data from Ermanyuk (2000), which were obtained at $H/D = 7.57$ and $N = 0.88$ rad s$^{-1}$, with the help of an 8-bit analog-to-digital convertor at the sampling frequency 12 Hz. Correspondingly, the scatter of the data is somewhat higher than in the present experiments.

The measured values of $C_\lambda(\Omega)$ at different $H/D$ are shown in figure 3. The data obtained in homogeneous water and shown in figure 2 are presented in figure 3 schematically by dash-dot, dash, dot and double-dot-dash lines. It is easy to see that at high frequency of oscillations ($\Omega > 1$) the damping is conditioned by viscous effects, which are quantitatively very close to those measured in the homogeneous water. When $\Omega < 1$, the radiation of energy with internal waves is the main mechanism of energy dissipation. As result, the damping coefficient $C_\lambda$ drastically increases compared to the value it takes in homogeneous water. However, as $H/D$ decreases, the portion of energy radiated with internal waves also decreases so that the viscous dissipation of energy becomes increasingly important. The drop of the radiated wave energy is most pronounced for the internal waves with nearly vertical vector of the group velocity (i.e. for $\Omega \to 1$). These waves undergo multiple reflections when travelling between the cylinder and the free surface (bottom). Thus, a certain portion of energy is 'trapped' in this region of space instead of being effectively radiated.

A qualitative theoretical description of this effect can be found within the framework of Gorodtsov & Teodorovich's (1986) approach with the important correction due to Voisin (2001*b*). Gorodtsov & Teodorovich (1986) derived an expression for the mean power radiated with internal waves by an arbitrary source of mass $q(\boldsymbol{x})$ in a stratified fluid. As the first approximation, they suggested modelling a circular

cylinder oscillating in a uniformly stratified fluid of infinite extent by the surface source obtained from the solution of the problem in an unbounded homogeneous fluid:

$$q(\boldsymbol{x}) = 2\boldsymbol{U} \cdot \frac{\boldsymbol{x}}{r}\hat{\delta}(r - \tilde{r}), \tag{4.2}$$

where $\hat{\delta}$ denotes the Dirac delta, $\boldsymbol{x} = (x, y)$, $\boldsymbol{U} = (U, V)$ is the velocity vector of the cylinder, $\tilde{r} = D/2$, and $r = (x^2 + y^2)^{1/2}$. The estimate of the mean radiated power obtained with this distribution does not agree with the theoretical results by Hurley (1997) or the measurements presented in Ermanyuk (2000). As found by Voisin (2001*b*), the correct form of the surface source is

$$q(\boldsymbol{x}) = 2\boldsymbol{U}^* \cdot \frac{\boldsymbol{x}}{r}\hat{\delta}(r - \tilde{r}) \tag{4.3}$$

with

$$U^* = [1 + (1 - \Omega^{-2})^{1/2}]\tfrac{1}{2}U,$$

$$V^* = [1 + (1 - \Omega^{-2})^{-1/2}]\tfrac{1}{2}W.$$

Note that for $\Omega < 1$ the values $U^*$ and $V^*$ are complex-valued. Substitution of the distribution (4.3) into the formula for wave power given in Gorodtsov & Teodorovich (1986) yields a result that exactly coincides with Hurley's (1997) solution for a circular cylinder oscillating in an unbounded uniformly stratified fluid, which, expressed in terms of the non-dimensional wave power $C_p = P(a^2\rho_c S N^3)^{-1}$, is

$$C_p = \tfrac{1}{2}\Omega^2(1 - \Omega^2)^{1/2}. \tag{4.4}$$

Gorodtsov & Teodorovich (1986) also derived an expression for the wave power radiated by an arbitrary source $q(\boldsymbol{x})$ in a uniformly stratified fluid of limited depth. The combination of this expression with the source (4.3) yields the following formulas for the non-dimensional wave power $C_p$ radiated by a circular cylinder oscillating at the depth $H/2$ in a linearly stratified fluid of depth $H$:

$$C_p = \Omega^2(1 - \Omega^2)^{1/2}A_{h,v}, \tag{4.5}$$

with $A_h = \sum_{n=0}^{\infty}(n + 1)^{-1}J_1^2((n + 1)K)$ and $A_v = \sum_{n=0}^{\infty}(n + 1/2)^{-1}J_1^2((n + 1/2)K)$ for the horizontal and vertical directions of oscillation, respectively, where $K = \pi(1 - \Omega^2)^{-1/2}D/H$ and $J_1$ is the Bessel function of the first order. It should be kept in mind that the use of the distribution (4.3) for a linearly stratified fluid of limited depth is just an approximation, which is appropriate only for sufficiently large $H/D$. Some details concerning the derivation of (4.4) and (4.5) are given in Appendix C.

Curves of (4.5) for the experimental values of $H/D$ are shown in figure 4 together with the experimental points. To separate the wave and viscous damping in experimental data we use an approach which is analogous to Froude's hypothesis for separation of wave and viscous components of ship resistance (see e.g. Newman 1977). The physical reason for the validity of this hypothesis is the difference between the characteristic length scales of wave and viscous phenomena. In the present problem, the thickness of the oscillatory boundary layer is of order $\delta_* \sim (\nu/\omega)^{1/2}$. The characteristic size of the internal wave pattern generated by the oscillating body is given by the width of the internal wave beams, which is of order $D$. The non-dimensional ratio of these parameters $\delta_*/D \sim \beta^{-1/2}$ is sufficiently small. Thus, the damping coefficient $\lambda(\omega)$ measured in experiments can be schematically represented as a sum of the wave damping $\lambda_w = C_\lambda^w \rho_c S N$ and the viscous damping $\lambda_v = C_\lambda^v \rho_c D(\omega\nu)^{1/2}$. Furthermore, we can assume that for a fixed geometry of the experiments $C_\lambda^w = f(\Omega)$ and $C_\lambda^v \approx$ const. It

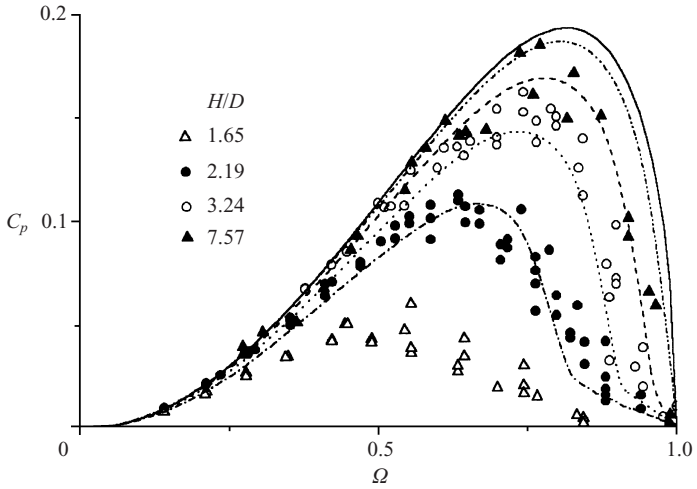


FIGURE 4. Non-dimensional radiated wave power $C_p$ vs. frequency $\Omega$ in linearly stratified fluid: solid line, formula (4.4) (Hurley 1997); other lines show calculations by formula (4.5) for $H/D = 1.65$ ($-\cdot-$), 2.19 ($\cdots$), 3.24 ($--$), 7.57 ($-\cdot\cdot-$).

should be kept in mind that the above assumptions constitute only a rough simplified scheme of the phenomena. On the physical level, wave and viscous effects in stratified fluids are interrelated in a rather complicated manner.

It follows from the data presented in figure 3 that $C_\lambda^v$ can be evaluated either from experiments in homogeneous water or from the data on $C_\lambda(\Omega)$ at $\Omega > 1$ (i.e. when $C_\lambda^w \equiv 0$). Within the accuracy of the experimental data, both estimates yield essentially the same result, which implies that, for practical purpose, we can take $C_\lambda^v \approx \Lambda/\beta^{1/2}$. Finally, in non-dimensional form

$$C_\lambda(\Omega) = C_\lambda^w(\Omega) + \frac{4}{\pi}\left(\frac{\Omega}{\beta_N}\right)^{1/2} C_\lambda^v. \tag{4.6}$$

It is apparent that the value $C_\lambda(\Omega)$ at given $\Omega$ is weakly sensitive to a small variation of $N$ since the second term in (4.6) is proportional to $N^{-1/2}$. Thus, in the present experiments the difference between the actual values of $N$ at different $H/D$ can be neglected.

The experimental points plotted in figure 4 represent the estimate of the non-dimensional radiated wave power

$$C_p(\Omega) = C_\lambda^w \Omega^2/2. \tag{4.7}$$

As is seen in figure 4, the approach, which uses the results by Gorodtsov & Teodorovich (1986) and Voisin (2001*b*), provides a consistent qualitative description of the main effect due to limited depth, i.e. the 'red shift' in the position of the maximum of the radiated wave power and the decrease of its magnitude. As might be expected, the quantitative agreement between theoretical and experimental results is good only for sufficiently large $H/D$, i.e. when (4.3) is applicable. At low $H/D$, the asymptotic formula (4.5) overestimates the power radiated with internal waves.

Values of $C_\mu(\Omega)$ measured at different $H/D$ are shown in figure 5. At low frequency the added mass coefficient $C_\mu$ is weakly dependent on $\Omega$. When the oscillation frequency exceeds a certain value $\Omega_0 < 1$, which is dependent on $H/D$, $C_\mu$ starts to grow and gradually approaches the asymptotic value for the homogeneous fluid of

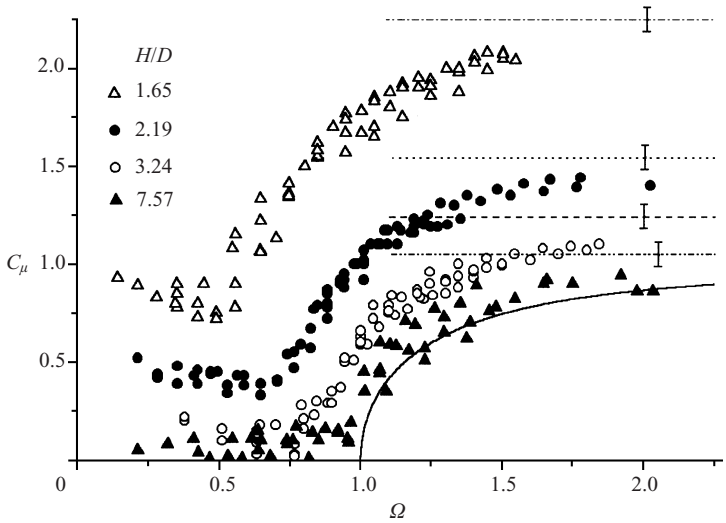


FIGURE 5. Added mass coefficient $C_\mu$ vs. frequency $\Omega$ in linearly stratified fluid: solid line, theory for $H/D = \infty$ (Hurley 1997); other lines show asymptotic values measured in homogeneous water for $H/D = 1.65$ (–·–), 2.19 (· · ·), 3.24 (– – –), 7.57 (– ·· –). Vertical bars denote the scatter of experimental data.

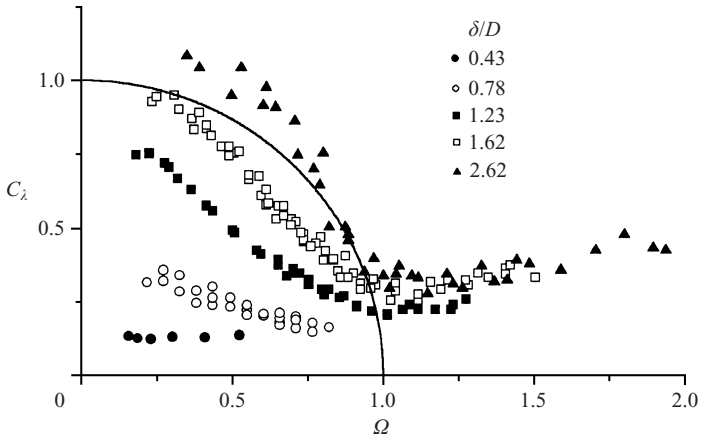


FIGURE 6. Damping coefficient $C_\lambda$ vs. frequency $\Omega$ in pycnocline at $\epsilon = 0.009$: solid line, Hurley (1997).

given depth. As the depth of fluid $H/D$ decreases, the non-dimensional frequency $\Omega_0$ shifts toward lower values. The asymptotic values of $C_\mu$ measured in homogeneous fluid at $H/D = 1.65$, 2.19, 3.24, 7.57 are marked in figure 5 by horizontal dash-dot, dash, dot and double-dot-dash lines, respectively. Recall that these values are systematically higher than the calculated estimates $C_\mu^{ideal}$ mentioned in § 4.1.

### 4.3. *Pycnocline*

The experiments in the stratified fluid with a pycnocline were carried out for three different values of relative difference of densities between the layers: $\epsilon = 0.003$, 0.006, 0.009. The total fluid depth in all the cases considered was $H = 28$ cm. The non-dimensional characteristic thickness of the pycnocline varied in the range

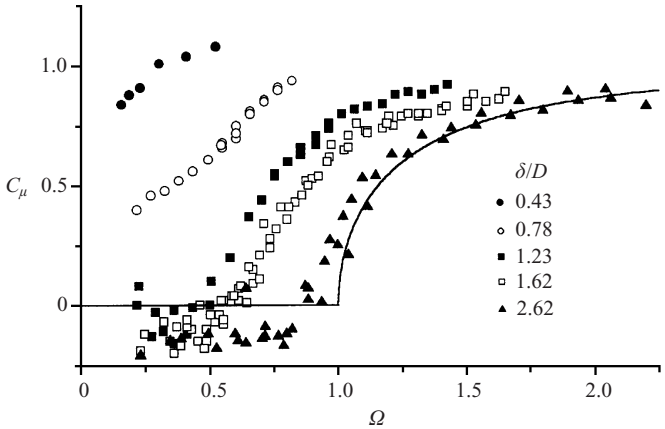


FIGURE 7. Added mass coefficient $C_\mu$ vs. frequency $\Omega$ in pycnocline at $\epsilon = 0.009$: solid line, Hurley (1997).

$0.43 \leqslant \delta/D \leqslant 2.62$. The measured values of $C_\lambda(\Omega)$ and $C_\mu(\Omega)$ are presented in figures 6 and 7 for $\epsilon = 0.009$. It is easy to see that at low $\delta/D$ the variation of the added mass coefficient $C_\mu$ with $\Omega$ is relatively small. $C_\mu$ is close to 1, i.e. to the value it takes in unbounded ideal homogeneous fluid. Correspondingly, the damping coefficient $C_\lambda$ and radiation of energy with internal waves are low. The viscous effects play the dominant role in the dissipation of energy. Note that the hydrodynamic loads on a cylinder oscillating at the interface of a two-fluid system (i.e. in the limiting case $\delta/D \to 0$) have not yet been studied theoretically. To the best of our knowledge, the existing studies are focused on the case when a body is entirely submerged in either the upper or lower layers of a two-fluid system (see e.g. Gorodtsov & Teodorovich 1986; Khabakhpasheva 1993; Sturova 1994). The dynamics of a body oscillating at the interface between two fluids is considered only in Akulenko & Nesterov (1987) and Akulenko *et al.* (1988), where the analysis is limited to the case of vertical oscillations of a vertical slender body. In the general case the problem is complicated by the effects at the contact line between the interface and the body surface. An experimental study closely related to the theoretical works by Akulenko & Nesterov (1987) and Akulenko *et al.* (1988) is described by Pyl'nev & Razumeenko (1991), who considered vertical oscillations of a thin vertical float in a continuously stratified fluid with a sharp pycnocline.

The increase of $\delta/D$ leads to the rapid growth of the wave radiation. As is apparent from figure 6, both the magnitude of the damping coefficient $C_\lambda$ and the range of non-dimensional frequencies $\Omega$ where it takes significantly high values increase with $\delta/D$. Accordingly (as follows from the Kramers–Kronig relations), the variation of $C_\mu$ with $\Omega$ becomes more and more pronounced. When $\delta/D = 2.62$ (see figures 6 and 7), the measured values of $C_\lambda(\Omega)$ and $C_\mu(\Omega)$ are already sufficiently close to the case of unbounded uniformly stratified fluid, as is evident from the comparison with the theoretical curves by Hurley (1997). It is interesting to note the occurrence of negative $C_\mu$ in figure 7. A similar effect is revealed in calculations of the added mass of a circular cylinder oscillating under the free surface of ideal homogeneous fluid (see Greenhow & Ahn 1988; Eatock Taylor & Hu 1991). In the present problem, there is no physical limitation on negative values of $C_\mu$; however $C_\lambda$ must be positive since the energy is radiated from the cylinder. As discussed by Greenhow & Ahn (1988) in the context of the Kramers–Kronig relations, negative $\mu(\omega)$ may occur in a frequency range where the drop of $\lambda(\omega)$ is sufficiently rapid (at the same time $\mu(\infty)$

should not be very large). Physically, this corresponds to a drastic drop of radiated wave energy, which is normally accompanied by the presence of standing waves in the vicinity of the cylinder. In the present problem these conditions occur in the pycnocline for internal waves with sufficiently large angle between the group velocity and the horizontal. Also, regarding functions $C_\mu(\Omega)$ and $C_\lambda(\Omega)$, one should keep in mind that, because of technical limitations, reliable experimental information for $\Omega \to 0$ could not be obtained. Hence the low-frequency asymptotic calls for further theoretical investigation.

The data obtained in the present experiments show that, if we are concerned with the dynamic effects in a real stratified fluid (natural stratification is usually characterized by the presence of a pycnocline), the popular approximation of a smooth pycnocline in the form of a two-fluid system with an interface between the layers is expected to be applicable only in a narrow range of low $\delta/D$. At the same time, another popular idealization, namely the model of unbounded uniformly stratified fluid, becomes appropriate and sufficiently accurate when $\delta/D \geqslant 2.6$. The intermediate range of $\delta/D$ studied in the present experiments seems to be the most complicated regarding a theoretical description, which of necessity should take into account the details of the distribution $N(y)$.

It might be appealing to extend the approximate approach described in § 4.2 to more general types of stratification, in particular to the case of a pycnocline. However, the success of Gorodtsov & Teodorovich (1986) in deriving analytical expressions for wave power radiated in uniformly stratified fluid of limited depth was conditioned by the very simple form of the eigenfunctions in that problem. In the case of a pycnocline the eigenfunctions of the problem are quite complicated (see Thorpe 1968). Hence, the derivation of analytic expressions similar to (4.5) is rather problematic. Alternatively, the case of pycnocline stratification can be investigated by numerical simulation. A recent numerical study of the hydrodynamic force acting on a cylinder oscillating in a pycnocline is given in Sturova (2001). In this study the pycnocline stratification is approximated as a three-fluid system with homogeneous upper and lower layers and a linearly stratified middle one. The cylinder is entirely submerged in the middle layer. Numerical results presented in Sturova (2001) seem to capture the main effects observed in the present experimental study. However, a detailed comparison shows some disagreements, which are, presumably, due to approximation of the real smooth pycnocline as a three-fluid system.

Experiments were also undertaken to study the effect of $\epsilon$ on $C_\lambda$ and $C_\mu$. When the characteristic pycnocline thickness $\delta$ varies due to natural diffusion, it is not easy to conduct an experiment at a fixed $\delta/D$ for different $\epsilon$. However, in the present experiments these data were obtained at $\delta/D = 1.23$ (with accuracy $\pm 2\%$) for $\epsilon = 0.003, 0.006, 0.009$, i.e. for the 'internal' Stokes numbers $\beta_N = 920, 1300, 1590$. The comparison of $C_\mu(\Omega)$ and $C_\lambda(\Omega)$ in this case is given in figure 8 and figure 9, respectively. The curves $C_\mu(\Omega)$ coincide with each other, which suggests that the 'inviscid scenario' plays the dominant role for the added mass. At the same time, damping coefficient $C_\lambda(\Omega)$ takes higher values for lower $\epsilon$ in accordance with (4.6). The second term in (4.6) is proportional to $N^{-1/2}$ or, equivalently, to $(\epsilon g/\delta)^{-1/4}$. Thus, although the experimental values of $\delta$ and $\epsilon$ varied within broad ranges, the effect of this variation on $C_\lambda(\Omega)$ is relatively weak. For example, when $\delta/D$ in experiments increased from 0.43 up to 2.62 ($\epsilon = 0.009$) the second term in (4.6) increased, roughly, by 60%. This estimate is in good agreement with the observed difference between $C_\lambda(\Omega)$ measured at different $\delta/D$ for $\Omega > 1$ as is seen in figure 6.

Using (4.6), the total damping can be decomposed into wave and viscous compo-

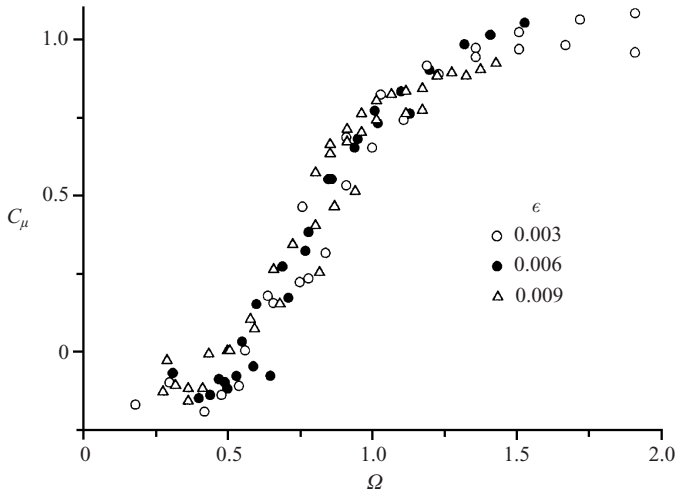


FIGURE 8. Added mass coefficient $C_\mu$ vs. frequency $\Omega$ in the pycnocline at $\delta/D = 1.23$ for different $\epsilon$.

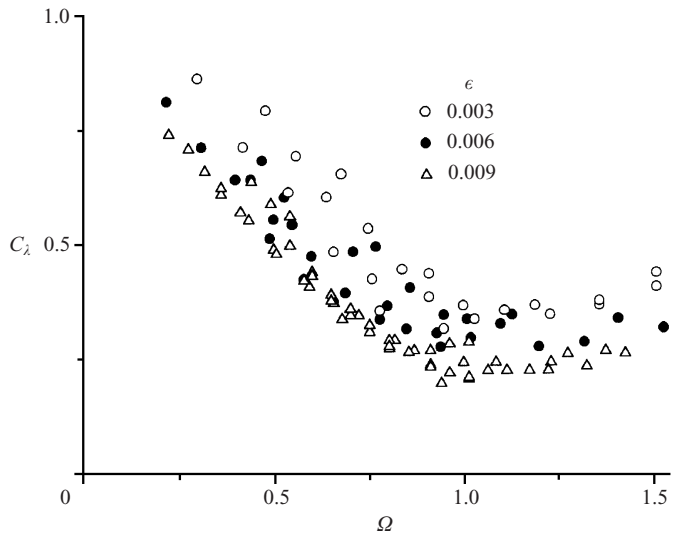


FIGURE 9. Damping coefficient $C_\lambda$ vs. frequency $\Omega$ in the pycnocline at $\delta/D = 1.23$ for different $\epsilon$.

nents. The result for the data shown in figure 9 is presented in figure 10 in terms of the non-dimensional radiated wave power $C_p(\Omega)$. As can be seen in figure 10, there is no systematic difference between the data obtained at different $\epsilon$, which supports the validity of decomposition (4.6). The effect of the pycnocline thickness on non-dimensional radiated wave power $C_p(\Omega)$ defined by (4.7) is illustrated in figure 11 for the data obtained at $\epsilon = 0.009$. The non-dimensional radiated wave power decreases with $\delta/D$ while the maximum of $C_p(\Omega)$ shifts toward lower values of $\Omega$. Thus, at least qualitatively, the effects of a finite vertical extent of stratification are similar for both cases of stratification considered in the present study, as is evident from the comparison of figure 4 and figure 11.

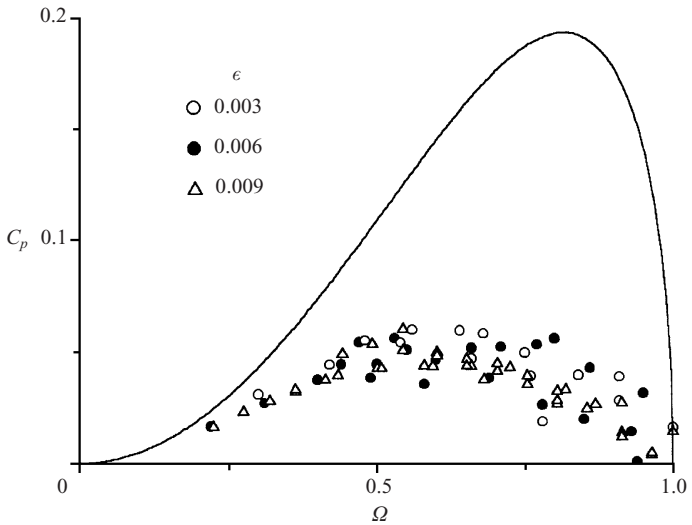


FIGURE 10. Non-dimensional radiated wave power $C_p$ vs. frequency $\Omega$ in the pycnocline at $\delta/D = 1.23$ for different $\epsilon$: solid line, formula (4.4) (Hurley 1997).

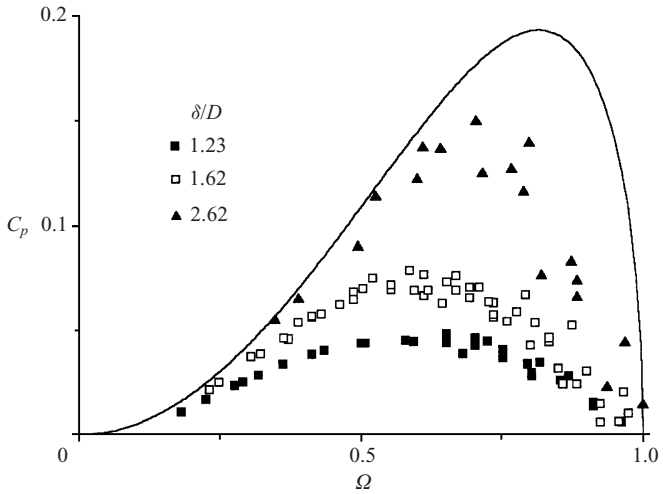


FIGURE 11. Non-dimensional radiated wave power $C_p$ vs. frequency $\Omega$ in the pycnocline at $\epsilon = 0.009$: solid line, formula (4.4) (Hurley 1997).

## 5. Concluding remarks

In this work we have applied the Fourier analysis of impulse response functions to evaluate experimentally the frequency-dependent added mass and damping of a circular cylinder oscillating horizontally in a continuously stratified fluid. The cases of the density distribution over depth studied include a linearly stratified fluid of limited depth and a pycnocline. It is shown that the density stratification has a strong effect on the force acting on an oscillating body. It is found that the main effect of a finite vertical extent of stratification (the depth of linearly stratified fluid or the pycnocline thickness) is to decrease the radiated wave power and to shift its maximum toward lower non-dimensional oscillation frequencies. The effect is most pronounced

at $\Omega \to 1$, i.e. for short waves with nearly vertical group velocity vector. For linearly stratified fluid of limited depth the difference between the maximum and minimum values of the added mass coefficient $C_\mu$ measured at fixed $H/D$ is about 1; it slightly increases for lower $H/D$. In a pycnocline, when $\delta/D$ is small, the variation of $C_\mu$ with $\Omega$ is small, so that for a nearly two-fluid system with an interface one can assume $C_\mu \approx 1$. As the pycnocline thickness $\delta/D$ increases, the measured values of $C_\mu(\Omega)$ gradually approaches the asymptotic case of unbounded uniformly stratified fluid (Hurley 1997).

It is also shown that for the range of parameters studied the total damping can be consistently decomposed into wave and viscous components. The viscous effects are found to be increasingly important at low values of fluid depth $H/D$ and 'internal' Stokes number $\beta_N$. The value of the added mass coefficient is essentially governed by an 'inviscid scenario'.

This study was supported by the Russian Foundation for Basic Research under grant No. 0001-00812 and by Siberian Branch of Russian Academy of Sciences (SB RAS) under grant No. 6 for young scientists and grant No. 1-2000 of Integration Project SB RAS. The authors express their gratitude to Professors I. V. Sturova and V. I. Bukreev for interesting discussions and encouragement. We also thank the referees for their clarifying and constructive comments, in particular for generous notes that greatly improved the presentation of analytic results.

## Appendix A. Equivalence of time-domain and frequency-domain solutions

Consider a circular cylinder of diameter $D$, mass per unit length $m$ and cross-sectional area $S$ floating in uniformly stratified fluid of infinite extent at the level of neutral equilibrium so that $m = \rho_c S$, where $\rho_c = \rho(y_c)$ is the fluid density at the vertical coordinate corresponding to the cylinder centre. Assume that the cylinder undergoes small harmonic vertical oscillations. The restoring force coefficient can be evaluated from hydrostatics as $c = -gS\,(\mathrm{d}\rho/\mathrm{d}y) = \rho_c S N^2$ (see Lai & Lee 1981 for a detailed discussion on decomposition of the fluid force into static and dynamic components). Then, for non-dimensional dynamic coefficients $C_\mu = \mu/\rho_c S$ and $C_\lambda = \lambda/\rho_c S N$, equations (2.5), (2.6) yield

$$C_\mu = \frac{1}{\Omega^2}\left[1 - \frac{R_c|R(0)|}{R_c^2 + R_s^2}\right] - 1, \tag{A 1}$$

$$C_\lambda = \frac{1}{\Omega}\frac{R_s|R(0)|}{R_c^2 + R_s^2}. \tag{A 2}$$

As found by Larsen (1969), the time-history $\zeta(t)$ of damped oscillations of a cylinder, initially held at the vertical distance $\zeta_0$ from the horizon of neutral buoyancy and then released with zero initial velocity, is described by the function $h(t) = \zeta(t)/\zeta_0 = J_0(Nt)$, where $J_0$ is the Bessel function of zeroth order, and the origin of the coordinate system is taken at the level of neutral equilibrium of the cylinder. This solution can be interpreted as the response to downward step loading, which is 'switched on' at $t = 0$. As follows from (2.1), the response function $r(t)$ to a positive unit impulse is related to $h(t)$ by time-differentiation $r(t) = -\mathrm{d}h(t)/\mathrm{d}t$. Thus, the impulse response function of a cylinder in uniformly stratified fluid is $r(t) = NJ_1(Nt)$. The Fourier

transform of the function $NJ_1(Nt)$ (see e.g. Ditkin & Prudnikov 1961) is

$$R_s = \frac{\omega}{(N^2-\omega^2)^{1/2}}, \quad R_c = 1 \quad \text{for } \omega < N,$$
$$R_s = 0, \quad R_s = 1 - \frac{\omega}{(\omega^2-N^2)^{1/2}} \quad \text{for } \omega > N.$$

By substituting these expressions in (A 1), (A 2) one can obtain $C_\mu \equiv 0$, $C_\lambda = (1-\Omega^2)^{1/2}$ for $\Omega < 1$ and $C_\mu = (1-\Omega^{-2})^{1/2}$, $C_\lambda \equiv 0$ for $\Omega > 1$, which exactly coincide with Hurley's results for a circular cylinder. There is no doubt that equivalence of time- (Larsen 1969) and frequency-domain (Lai & Lee 1981) solutions for a sphere can be proven in similar manner. In the latter case, we restricted ourselves to a numerical check of the equivalence by a version of the computer programme that was used in the present study for the processing of experimental data.

## Appendix B. Kramers–Kronig relations for Hurley's (1997) solution

The validity of formulas (2.7), (2.8) for Hurley's (1997) solution can be verified by residue calculus. Taking into account the finite spectrum of internal waves ($\Omega \leqslant 1$), (2.7) can be rewritten in non-dimensional form as

$$C_\mu(\Omega) - C_\mu(\infty) = \frac{2}{\pi}\int_0^1 (1-\xi^2)^{1/2}\frac{\mathrm{d}\xi}{\xi^2-\Omega^2}, \tag{B 1}$$

where the non-dimensional force coefficients are defined the same way as in Appendix A and in equations (2.10), (2.11) of the main body of the paper.

Keeping in mind that $\mu(\omega)$ and $\lambda(\omega)/\omega$ are even and uneven functions of $\omega$, respectively, the integral in (B 1) can be represented as the integral along the unit circle $C$ by substituting $\xi = \frac{1}{2}(z+1/z)$:

$$\int_0^1 (1-\xi^2)^{1/2}\frac{\mathrm{d}\xi}{\xi^2-\Omega^2} = -\frac{1}{4\mathrm{i}}\int_C \frac{(z^4-2z^2+1)\,\mathrm{d}z}{[z^4+2(1-2\Omega^2)z^2+1]z}.$$

The evaluation of this integral is a straightforward application of residue calculus. It yields $C_\mu(\Omega) = 0$ for $\Omega < 1$ and $C_\mu = (\Omega^2-1)^{1/2}/\Omega$ for $\Omega > 1$, as expected. The validity of (2.8), which in the present problem takes the form

$$C_\lambda(\Omega) = -\frac{2}{\pi}\Omega^2\int_0^\infty [C_\mu(\xi)-1]\frac{\mathrm{d}\xi}{\xi^2-\Omega^2} + 1,$$

can be proven in a similar manner.

The integral (2.9) can be evaluated via residue calculus as the integral for the function $\mu(\omega) - \mathrm{i}\lambda(\omega)/\omega$ in the lower half-plane along a closed contour, which consists of the real axis with a small indentation at $\omega = 0$ and the infinitely large semicircle. In non-dimensional form, for Hurley's (1997) solution the integration yields non-zero value

$$\int_0^\infty [C_\mu(\Omega) - C_\mu(\infty)]\,\mathrm{d}\Omega = -\frac{\pi}{2}.$$

## Appendix C. Calculation of mean radiated wave power

According to Gorodtsov & Teodorovich (1986), the mean power radiated by a two-dimensional source of mass $q(\boldsymbol{x})\exp(\mathrm{i}\omega t)$ in a uniformly stratified fluid of infinite

extent is

$$P = \frac{\rho_c \omega (N^2 - \omega^2)}{8\pi} \int \mathrm{d}^2 k |q(\boldsymbol{k})|^2 \, \hat{\delta}(\omega^2 \zeta^2 - N^2 k^2), \tag{C 1}$$

where $\boldsymbol{k} = (k, l)$ are the wavenumber vectors satisfying the dispersion relation $\omega^2\zeta^2 - N^2k^2 = 0$, with $\zeta = (k^2 + l^2)^{1/2}$, and $q(\boldsymbol{k})$ is the spatial spectrum

$$q(\boldsymbol{k}) = \int q(\boldsymbol{x}) \exp(\mathrm{i}\boldsymbol{k} \cdot \boldsymbol{x}) \, \mathrm{d}^2 x.$$

Integral (C 1) evaluates to

$$P = \frac{\rho_c N}{8\pi} (1 - \Omega^2)^{1/2} \int_0^\infty \frac{\mathrm{d}\zeta}{\zeta} |q[\zeta\Omega, \pm\zeta(1 - \Omega^2)^{1/2}]|^2. \tag{C 2}$$

With the source (4.2) formula (C 2) yields Gorodtsov's & Teodorovich's (1986) result for wave power

$$P = \tfrac{1}{2}\pi\rho_c N D^2 (1 - \Omega^2)^{1/2} [U^2\Omega^2 + V^2(1 - \Omega^2)]$$

With the source (4.3), we have

$$P = \tfrac{1}{8}\pi\rho_c N D^2 (1 - \Omega^2)^{1/2} (U^2 + V^2), \tag{C 3}$$

which, in non-dimensional form, amounts to (4.4). Note that for fixed amplitude of oscillations the radiated wave power given by (C 3) does not depend on the direction of oscillations in agreement with Hurley (1997).

For variable buoyancy frequency $N(y)$ or finite fluid depth $H$, internal waves propagate horizontally along the wave guide as a sum of vertical modes. Each mode with index $n$ is characterized by the dispersion relation $\omega_n(k)$ and the eigenfunction $\phi_n(k, y)$. The eigenfunctions are orthogonal and normalized in such a way that

$$\int_{-H}^0 N^2(y) \phi_n(k, y) \phi_m(k, y) \, \mathrm{d}y = \delta_{nm},$$

where $\delta_{nm}$ is the Kronecker delta. In this case Gorodsov & Teodorovich (1986) give the following expression for the wave power:

$$P = \frac{\rho_c \omega^3}{4} \int \frac{\mathrm{d}k}{k^4} \sum_n \left| \int_{-H}^0 q(k, y) \frac{\partial \phi_n}{\partial y}(k, y) \, \mathrm{d}y \right|^2 \hat{\delta} \left[ \frac{\omega^2}{\omega_n^2(k)} - 1 \right].$$

For constant $N$ and finite $H$ the eigenfunctions are sinusoidal and the wave power is given by

$$P = \frac{\rho_c N}{8\pi} (1 - \Omega^2)^{1/2} \sum_{n=1}^\infty \frac{1}{n} \left| \sum_{\pm} q \left[ \frac{n\pi}{H} (\Omega^{-2} - 1)^{-1/2}, \pm \frac{n\pi}{H} \right] \right|^2.$$

For an oscillating circular cylinder located at depth $y_0$ and represented by the source (4.2), with $y$ replaced by $y + y_0$, Gorodtsov & Teodorovich (1986) obtained the following estimate:

$$P = 2\pi\rho_c N D^2 (1 - \Omega^2)^{1/2} \sum_{n=1}^\infty \frac{1}{n} J_1^2(\tfrac{1}{2}nK) \left[ U^2\Omega^2 \cos^2 \left( n\pi \frac{y_0}{H} \right) + V^2(1 - \Omega^2) \sin^2 \left( n\pi \frac{y_0}{H} \right) \right].$$

For the source (4.3) we have instead

$$P = \tfrac{1}{2}\pi\rho_c N D^2 (1-\Omega^2)^{1/2} \sum_{n=1}^{\infty} \frac{1}{n} J_1^2(\tfrac{1}{2}nK) \left[ U\cos\left(n\pi\frac{y_0}{H}\right) + V\sin\left(n\pi\frac{y_0}{H}\right)\right]^2. \quad (C\,4)$$

In non-dimensional form for $y_0 = -H/2$ and purely horizontal or vertical direction of cylinder oscillations the formula (C 4) reduces to (4.3). Formulas (C 3) and (C 4) for an arbitrary direction of oscillation were kindly pointed out to the authors by one of the referees; initially their consideration was restricted to purely horizontal or vertical oscillations.

## REFERENCES


Akulenko, L. D., Mikhailov, S. A., Nesterov, S. V. & Chaikovsky, A. A. 1988 Numerical-analytic investigation of oscillations of a rigid body at the interface between two liquids. *Mech. Solids* **23**, 54–60.

Akulenko, L. D. & Nesterov, S. V. 1987 Oscillations of a solid at the interface between two fluids. *Mech. Solids* **22**, 30–36.

Appleby, J. C. & Crighton, D. G. 1986 Non-Boussinesq effects in the diffraction of internal waves from an oscillating cylinder. *Q. J. Mech. Appl. Maths* **39**, 209–231.

Appleby, J. C. & Crighton, D. G. 1987 Internal gravity waves generated by oscillations of a sphere. *J. Fluid Mech.* **183**, 439–450.

Arntsen, Ø. A. 1996 Disturbances, lift and drag forces due to translation of a horizontal circular cylinder in stratified water. *Exps. Fluids* **21**, 387–400.

Castro, I. P., Snyder, W. N. & Baines P. G. 1990 Obstacle drag in stratified flow. *Proc. R. Soc. Lond.* A **429**, 119–140.

Cummins, W. E. 1962 The impulse response function and ship motions. *Schiffstechnik* **9**, 101–109.

Dalziel, S. B., Hughes, G. O. & Sutherland, B. R. 2000 Whole-field density measurements by 'synthetic schlieren'. *Exps. Fluids* **28**, 322–335.

Ditkin, V. A. & Prudnikov, A. P. 1961 Integral transforms and operational calculus. *Gos. Izd. Fiz.-Mat. Lit. Moscow* (in Russian).

Eatock Taylor, R. & Hu, C. S. 1991 Multipole expansions for wave diffraction and radiation in deep water. *Ocean Engng* **18**, 191–224.

Ermanyuk, E. V. 2000 The use of impulse response functions for evaluation of added mass and damping coefficient of a circular cylinder oscillating in linearly stratified fluid. *Exps. Fluids* **28**, 152–159.

Gorodtsov, V. A. & Teodorovich, E. V. 1986 Energy characteristics of harmonic internal wave generators. *J. Appl. Mech. Tech. Phys.* **27**, 523–529.

Greenhow, M. & Ahn, S. I. 1988 Added mass and damping of horizontal circular cylinder sections. *Ocean Engng* **15**, 495–504.

Hurley, D. G. 1969 The emission of internal waves by vibrating cylinders. *J. Fluid Mech.* **36**, 657–672.

Hurley, D. G. 1997 The generation of internal waves by vibrating elliptic cylinders. Part 1. Inviscid solution. *J. Fluid Mech.* **351**, 105–118.

Hurley, D. G. & Keady, G. 1997 The generation of internal waves by vibrating ellipotic cylinders. Part 2. Approximate viscous solution. *J. Fluid Mech.* **351**, 119–139.

Ivanov, A. V. 1989 Generation of internal waves by an oscillating source. *Izv. Atmos. Ocean. Phys.* **25**, 61–64.

Kerwin, J. E. & Narita, H. 1965 Determination of ship motion parameters by a step response technique. *J. Ship Res.* **9**, 183–189.

Khabakhpasheva, T. I. 1993 Diffraction of internal waves on cylinder in two-layer fluid. *Atmos. Ocean Phys.* **29**, 559–564.

Kistovich, A. V. & Chashechkin, Yu. D. 1995 Reflection of packets of internal waves from a rigid plane in a viscous fluid. *Izv. Atmos. Ocean. Phys.* **30**, 718–724.

Kotik, J. & Mangulis, V. 1962 On the Kramers–Kronig relations for ship motions. *Intl Shipbuilding Prog.* **9**, 351–368.

Lai, R. Y. S. & Lee, C.-M. 1981 Added mass of a spheroid oscillating in a linearly stratified fluid. *Intl J. Engng Sci.* **19**, 1411–1420.

Landau, L. D. & Lifshitz, E. M. 1980 *Statistical Physics*. Part 1. Butterworth–Heinemann.

Landau, L. D. & Lifshitz, E. M. 1987 *Fluid Mechanics*. Butterworth–Heinemann.

Larsen, L. H. 1969 Oscillations of a neutrally buoyant sphere in a stratified fluid. *Deep-Sea Res.* **16**, 587–603.

Lofquist, K. E. & Purtell, L. P. 1984 Drag on a sphere moving horizontally through a stratified fluid. *J. Fluid Mech.* **148**, 271–284.

Makarov, S. A., Neklyudov, V. I. & Chashechkin, Yu. D. 1990 Spatial structure of two-dimensional monochromatic internal-wave beams in an exponentially stratified liquid. *Izv. Atmos. Ocean. Phys.* **26**, 548–554.

McIver, P. & Linton, C. M. 1991 The added mass of bodies heaving at low frequency in water of finite depth. *Appl. Ocean. Res.* **13**, 12–17.

Mowbray, D. E. & Rarity, B. S. H. 1967 A theoretical and experimental investigation of the phase configuration of internal waves of small amplitude in a density stratified liquid. *J. Fluid Mech.* **28**, 1–16.

Newman, J. N. 1977 *Marine Hydrodynamics*. MIT Press.

Newman, J. N. 1978 The theory of ship motions. *Adv. Appl. Mech.* **18**, 221–283.

Nicolaou, D., Liu, R. & Stevenson, T. N. 1993 The evolution of thermocline waves from an oscillatory disturbance. *J. Fluid Mech.* **254**, 401–416.

Nikitina, E. A. 1959 Ship resistance in 'dead water'. *Izv. Akad. Nauk SSSR, OTN Mekh. i Mashinostroenie* **1**, 188–192.

Pyl'nev, Yu. V. & Razumeenko, Yu. V. 1991 Damped oscillations of a float of special shape, deeply immersed in a homogeneous and stratified fluid. *Mech. Solids* **26**, 67–76.

Sarpkaya, T. 1986 Force on a circular cylinder in viscous oscillatory flow at low Keulegan–Carpenter numbers. *J. Fluid Mech.* **165**, 61–71.

Shishkina, T. 1996 Comparison of the drag coefficients of bodies moving in liquids with various stratification profiles. *Fluid Dyn.* **31**, 484–489.

Stokes, G. G. 1851 On the effect of the internal friction of fluids on the motion of pendulums. *Trans. Camb. Phil. Soc.* **9**, 8–106.

Sturova, I. V. 1994 Plane problem of hydrodynamic rocking of a body submerged in a two-layer fluid without forward speed. *Fluid Dyn.* **29**, 414–423.

Sturova, I. V. 2001 Oscillations of a circular cylinder in a layer of linearly stratified fluid. *Fluid Dyn.* **36**, 478–488.

Sutherland, B. R., Dalziel, S. B., Hughes, G. O. & Linden, P. F. 1999 Visualization and measurement of internal waves by 'synthetic schlieren'. Part 1. Vertically oscillating cylinder. *J. Fluid Mech.* **390**, 93–126.

Thorpe, S. A. 1968 On the shape of progressive internal waves. *Phil. Trans. R. Soc. Lond.* A **263**, 563–614.

Turner, J. S. 1973 *Buoyancy Effects in Fluids*. Cambridge University Press.

Voisin, B. 1991 Internal wave generation in uniformly stratified fluids. Part 1. Green's function and point sources. *J. Fluid Mech.* **231**, 439–480.

Voisin, B. 2001*a* Oscillating bodies and added mass for internal gravity waves. Part 1. Spheres. *J. Fluid Mech.* (in preparation).

Voisin, B. 2001*b* Oscillating bodies and added mass for internal gravity waves. Part 2. Circular cylinders. *J. Fluid Mech.* (in preparation).

Wang, C.-Y. 1968 On high-frequency oscillating viscous flows. *J. Fluid Mech.* **32**, 55–68.

Wehausen, J. V. 1971 The motion of floating bodies. *Annu. Rev. Fluid Mech.* **3**, 237–268.